Çanakkale Onsekiz Mart University

Journal of Advanced Research in Natural and Applied Sciences

dergipark.org.tr/tr/pub/jarnas

Open Access

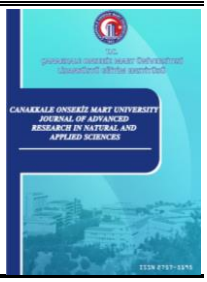

e-ISSN: 2757-5195 2024, Vol. 10, Issue 2, Pages: 272-284 doi.org/10.28979/jarnas.1350766

Optical and Electrical Characterization of Crystallized M:WO_3 (Cu, Fe, Ni) Films in Acidic Medium

Emin Yakar[1], Irmak Karaduman Er[2], Fatma Sarf[3]

[1]Department of Materials Science and Engineering, Faculty of Engineering, Çanakkale Onsekiz Mart University, Çanakkale, Türkiye
[2]Department of Medical Services and Techniques, Eldivan Medical Services Vocational School, Çankırı Karatekin University, Çankırı, Türkiye
[3]Çan Vocational School, Çanakkale Onsekiz Mart University, Çanakkale, Türkiye

Article History

Received: 27 Aug 2023

Accepted: 21 Nov 2023

Published: 25 Jun 2024

Research Article

Abstract − Pure and metal (M) doped [copper (Cu), nickel (Ni) and iron (Fe)] WO_3 films have been produced on In:SnO_2 (ITO) slides by using facile chemical bath deposition and then annealed at 500 ºC for 2 h. Structural, morphological, electrical and optical properties of the produced WO_3-based films were examined. Monoclinic WO_3 phase were observed in all the samples, and the peak intensities were decreased by metal inclusion with heterogeneous film growth on ITO substrate. Slight shifts from defect related emission peaks (blue and green) were observed in metal-substituted WO_3 samples from PL study. An optical band gap was observed to decrease in M:WO_3 samples. The surface resistance values were significantly reduced by metal additives compared to its pure counterpart, especially by the inclusion of nickel ions in WO_3. The results indicated that nucleus growth and thereby impurity/defect-related surfaces had a serious effect on the optical and electrical properties of M:WO_3 films.

Keywords − *Chemical bath deposition, electrical, optical, WO_3 film*

1. Introduction

In the past decade, metal oxide semiconductor structures of all dimensions (0D, 1D, 2D and 3D) have been often studied to use in many technological fields such as gas sensors [1], supercapacitors [2], solar cells [3] and magnetic memory devices [4]. Thanks to their numerous advantages, they have been proposed as an alternative to silicon-based technology. Regardless of the technological field in which it is used, properties of metal oxides such as low cost, abundance in nature, simple production, high chemical stability and versatile approach have stood out [5]. In order to find their advanced applications, it is important to understand these materials by conducting extensive research. Improvement in the using field is mostly achieved by low concentration of elements or oxygen vacancy doping [6] and hetero-/homojunction construction with adding C-based material [7] which have a high impact on the crystal growth and surface forms.

As an unique metal oxide material, tungsten trioxide (WO_3) has an oxygen-deficient n-type wide band gap of around 2.6-3 eV, high work function, enhanced specific surface area and the fast recombination of photogenerated electron-hole pairs of WO_3 [8,9]. The compounds between tungsten and oxygen are quite numerous and complex. For example, in fully oxidized tungsten oxide compounds, W metal gets +6 valency and forms 4 octahedrons with oxygen.

With its gradually improving optical and electrical properties, different type WO_3 structures (nanorods,

[1]eyakar@comu.edu.tr (Corresponding Author); [2]irmakkaradumaner@karatekin.edu.tr; [3]fatmaozutok@comu.edu.tr

nonosheets, thin films) were synthesized for a variety of applications such as photodedectors [10], organic light emitting diodes [11], electrochromic devices [12], and optoelectronic devices [13]. The choice of WO_3 production method is so important to obtain desired structures.

Among the thin film production methods, the chemical bath deposition provides the ability to be applied to large surfaces and allows the production of the necessary topographic, physical and crystallographic structures by making the necessary deposition optimization (solution type, precursor molarity, working temperature and etc.) [14]. Through the homogeneous or heterogeneous growth process could be controlled, the final product could be easily fabricated. For example, $H_2C_2O_4$ was used as a growth controller to regulate the growth process of the H_2WO_4 film formed on FTO substrate. Hence, three steps were proposed for homogeneous nanosheet WO_3 thin film growth by controlling the reactants amount [15].

It has been stated that film quality (adherency, thickness, homogeneous surface etc.) is mostly dependent on film production, which significantly affects the film growth process in many studies [16]. Among chemical type film production techniques (dip coating, chemical vapor deposition, spin coating etc.) chemical bath deposition is so attractive with its simplicity, no set-up and ability to expand to large surfaces

There are a lot of studies realized about hetero-atom doped WO_3 films [17]. In solar cell applications, element-doped WO_3 could promoting photocatalytic activity by extending the solar light response range and inhibiting the recombination of photogenerated charge carriers [18]. As a gas sensor sensing layer, 1 wt% Pt:WO_3 sensor exhibited quite low detection limit of 100 ppb at optimum operating temperature of 160 °C [19]. Binary metal components were dispersed into each other, which contributed to promoting the metal/metal electron interaction and adjusting the physicochemical properties of mixed metal oxides, according to transition metal doped WO_3 mixed oxides study of Chen et.al [20].

In this paper, we discuss the metal inclusion (Cu, Fe and Ni) effect on the electrical and optical properties of WO_3 films depending on changing surface morphology and lattice structure.

2. Materials and Methods

In this study, facile chemical bath deposition was used to produce M:WO_3 films and detailed production stages was explained in our previous study [21]. The chemicals used in the preparation of films were of high quality and purity (Sigma Aldrich, 99.9 %). Tungsten and metal sources were sodium tungsten dihydrate, nickel acetate tetrahydrate, iron chloride hexahydrate and copper acetate dihydrate.

All WO_3 films were coated on to In:SnO_2 (ITO) substrates after standard substrate cleaning. In 100 ml distilled water, homogenous aqueous solutions were obtained under Table 1 conditions to obtain different type metal doped WO_3 films. Complex agent (HCl) was added drop by drop and pH was kept constant throughout the experiment. Films were prepared in harsh acidic medium unlike a similar study to observe film growth process [22]. The pH value of the solution was 2 at room temperature. Finally, all films were annealed in air furnace under Table 1 condition.

Structural and morphological properties were investigated by X-ray powder diffraction (XRD; Rigaku Smart Lab x-ray diffractometer; CuKα radiation; 45 kV; 40 mA; step size 0.013º) and scanning electron microscopy (SEM; JEOL JSM- 7100F; Au-Pd ratio of 80-20 %), respectively. WO_3 thin films with and without additives coated on IDT, whose properties will be determined, were fixed on an aluminum substrate with 1×3 cm dimensions and 1 mm thickness. Thin films fixed on the aluminum substrate are placed in the measuring cell made of aluminum. The electrical contacts between the sample and the measuring cell are made using liquid

silver. The thickness was estimated by the weight difference method which is given our previous study [23]. The thickness of WO_3, Ni-doped WO_3, Fe-doped WO_3 and Cu-doped WO_3 were calculated as 800 nm, 500 nm, 600 nm and 930 nm, respectively.

Table 1. Deposition parameters of WO_3 films

Parameters	Values
pH	2
Working temperature	70±5 °C
Bath time	15 min.
Annealing temperature	500 °C
Annealing time	2 h

3. Results and Discussion

Figure 1 shown the 3D-AFM topography of synthesized WO_3 samples. It is clearly seen that the surface roughness has increased with nickel inclusion. Surface roughness (root-mean-square (rms)) values were 93.8-142 nm range for produced samples. Thick and heterogenous distribution particle on the substrate by metal inclusion indicates that the attraction force between the different metal atoms might increase and agglomerative or cluster forms might be occurs.

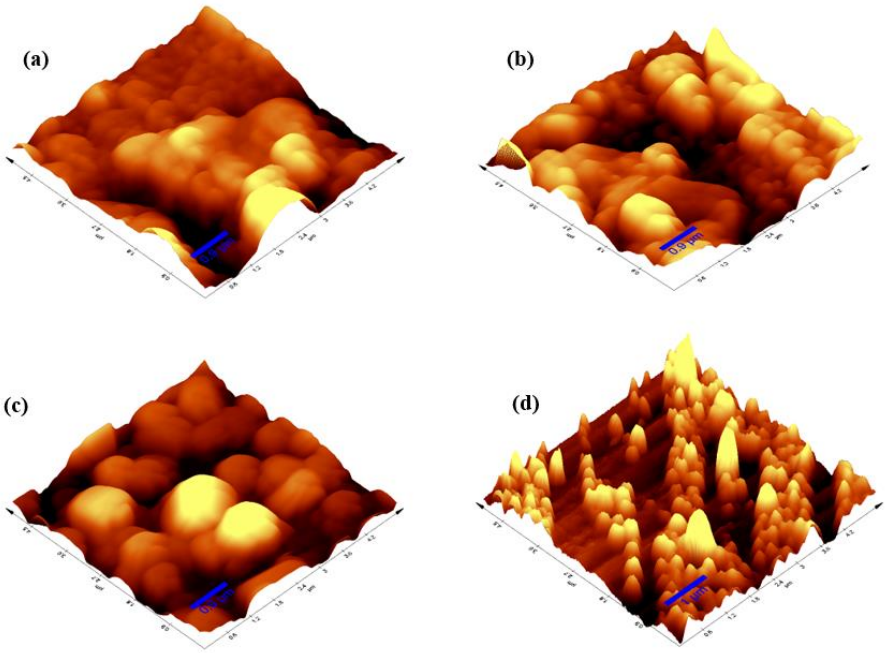

Figure 1. The AFM images of WO_3 (a), Cu:WO_3 (b), Fe:WO_3 (c) and Ni: WO_3(d)

Figure 2 depicted the x-ray diffraction peaks of WO_3 samples. Characteristic three monoclinic WO_3 polycrystalline phase peaks of (001), (020) and (200) were seen according to JCPDS Card No: 43-1035 [24]. ITO-based peak and W-related peak are observed in the 2θ= 65-70 and 2θ= 45°-50° range, respectively due to less crystal nuclei in harsh acidic medium and low adhesion of coating film on ITO [21,25]. The material with the significant change crystallization is the WO_3 sample with nickel included due to heterogeneous growth (caused by low dissolution of Ni-source) on ITO surface. The crystalline size were calculated by Debye-Scherrer equation from the below formula;

$$D = \frac{k\lambda}{\beta \cos\theta} \tag{3.1}$$

In Equation (3.1.), k is a numerical factor frequently referred to as the crystallite-shape factor, λ is the wavelength of the X-rays, β is the width (full-width at half-maximum) of the X-ray diffraction peak in radians and θ is the Bragg angle. The average crystalline size of the produced samples was calculated according to the preferred orientation of (110). The average crystalline size of samples was calculated 136, 133, 87 and 16 nm for pure WO_3, Fe:WO_3, Cu:WO_3 and Ni.WO_3, respectively. Apart from the peaks related to the substrate and tungsten, no second phase has been found. It indicates that metal atoms were placed in the host WO_3 structure however defects have enormous effect on the host lattice with shifting of typical WO_3 peaks which may be attributed to the development of additional growth centers by metal inclusion [26, 27]. Ionic radius of W^{6+}, Cu^{2+}, Fe^{2+} and Ni^{2+} are 62 nm [28], 73 nm [29], 64 nm [28], and 69 nm [24], ionic radius of selected metal atoms is higher than tungsten ionic radius. This may cause it difficult to replacement of W-M ions and thereby lattice damage increases.

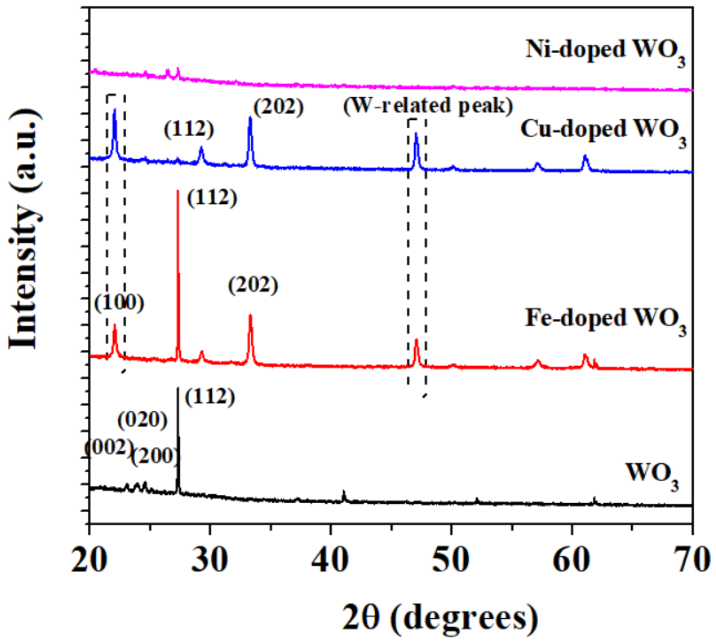

Figure 2. The x-ray diffraction (XRD) peak analysis of the produced pure and M:WO_3 films

To study the influence of defects in WO_3 host lattice photoluminescence (PL) was performed and PL spectra is deconvoluted into multi peaks with using Gaussian fitting. Figure 3 shows the PL analysis of pure and M:WO_3 films. A series of peaks are detected at 428, 427,429, 523, 560 and 687 nm which may be attributed to surface defects. It is clear that these emissions may be predicted by the recombination of free excitons [30]. Furthermore, it is interesting to find that the intensity of light in the range of 510-687 nm changes with the hetero-crystal growth. Blue emission peak at around 428 nm and green emission peak approximately at 523 nm were observed in pure WO_3, which correlated to similar studies [27]. Emission peaks broadening and shifting were observed in metal included WO_3 samples (especially in Ni:WO_3 sample) due to recombination of electron-hole pairs attributed to oxygen vacancies, self-trapped excitons states and surface defects/states [31,32].The PL peak intensity of WO_3 is increased by copper inclusion with a similar crystal structure of host WO_3.

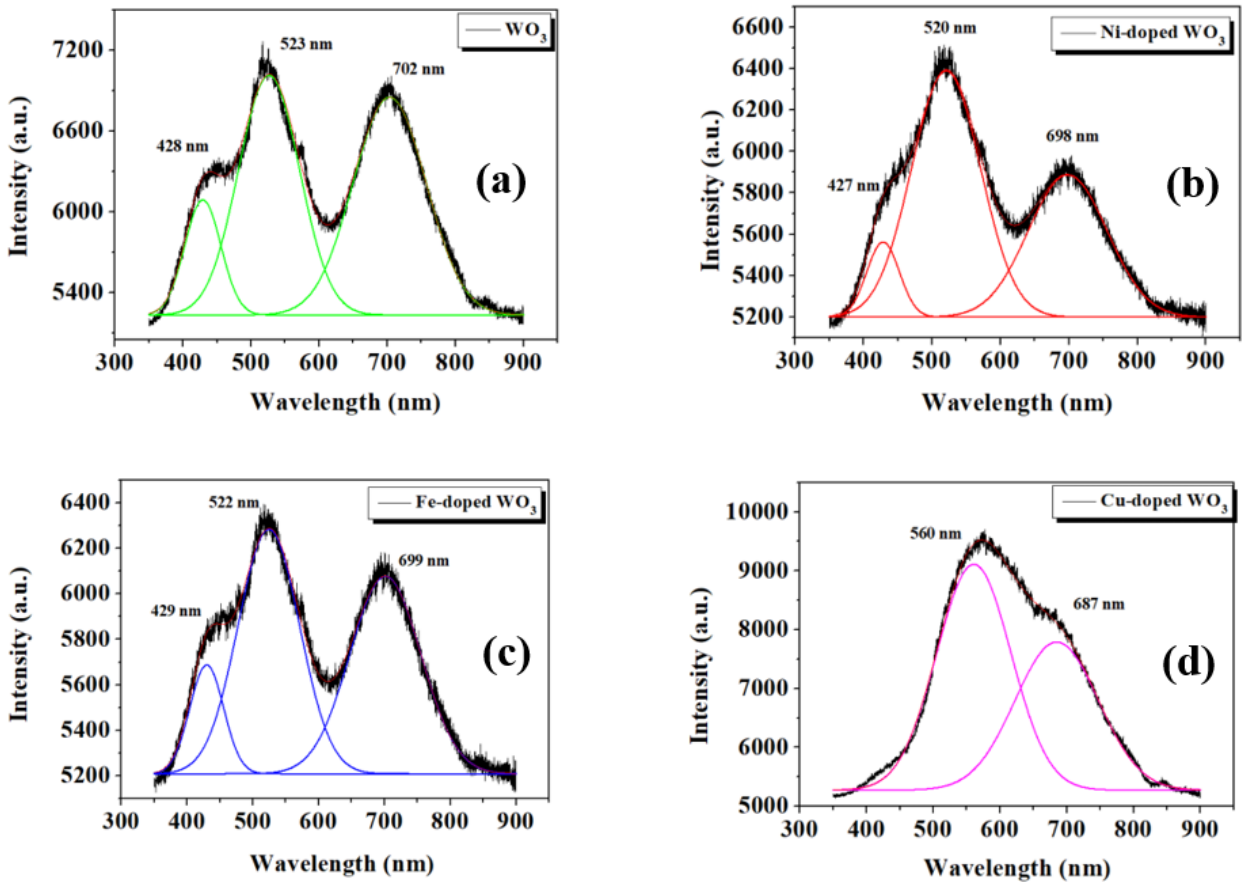

Figure 3. The PL analysis of WO_3 (a), Ni: WO_3 (b), Fe:WO_3 (c) and Cu:WO_3 (d)

Figure 4 and Figure 5 exhibited the UV-Vis spectra in the 200-800 nm range and the optical band gap of the samples, respectively. The broad optical absorption band in the optical transmittance spectrum of the deposited WO_3 film is attributed to the presence of tungsten (W^{4+}) ions [33]. It is clear that optical parameters have been affected by film thickness, surface topography, crystal quality etc. Optical band edge shifted higher wavelength by iron inclusion and defect-related second optical absorption edge was observed in WO_3, Ni:WO_3 and Cu:WO_3. The low crystal quality in the WO_3 host lattice and the metal-tungsten interstitial location may be the reason why pure WO_3 changes its optical character.

The optical band gap estimated by extrapolating the straight-line portion of the $(\alpha h\nu)^2$ vs $h\nu$ plot for WO_3 samples. The optical band gap was calculated by using the below Tauc plot [34, 35]:

$$\alpha = \frac{A(h\upsilon - E_g)^n}{h\vartheta} \tag{3.2}$$

where A is a constant and n is an index for allowed direct and non-direct transitions are 1/2 and 2, respectively. In our study, the band gap of both undoped and doped TiO_2 films were obtained by considering the direct (1/2) transition since it is more favorable for anatase TiO_2 according to the reported studies of Reddy et.al. [34] and Devi et.al. [35].

The thickness was estimated by the weight difference method which is given our previous study [23]. The thickness of WO_3, Ni-doped WO_3, Fe-doped WO_3 and Cu-doped WO_3 were calculated as 800 nm, 500 nm, 600 nm and 930 nm, respectively.

The optical band gap of WO_3, Ni:WO_3, Fe:WO_3 and Cu:WO_3 were calculated 2.92 eV, 2.79 eV, 2.87 eV and 2.78 eV, respectively. Optical band gap decrease was shown by metal inclusion which correlated to change of crystalline size [36, 37]. Metal inclusion of pure WO_3 may cause lattice damage which induces the defect energy levels below the conduction band causes the decrease of optical band gap [38]. In our previous study, the indirect bandgap energies of the nickel doped WO_3 films were found as 3.36 eV-2.74 eV range with using different type nickel precursors and optical band gap decrease was also observed as in this study [36].

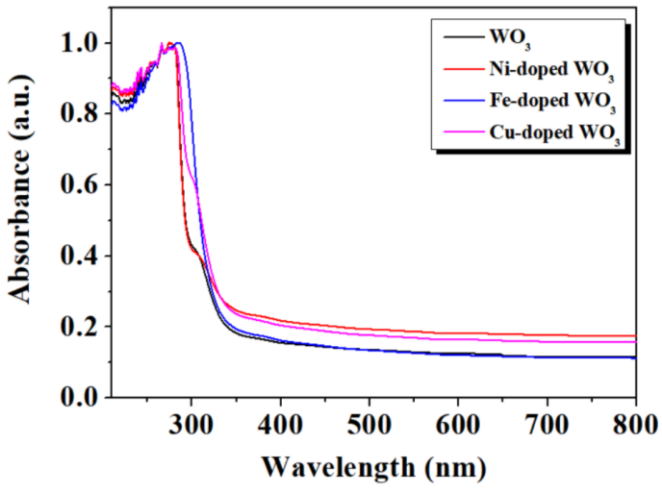

Figure 4. UV-Vis spectra of pure WO_3 and M:WO_3 films

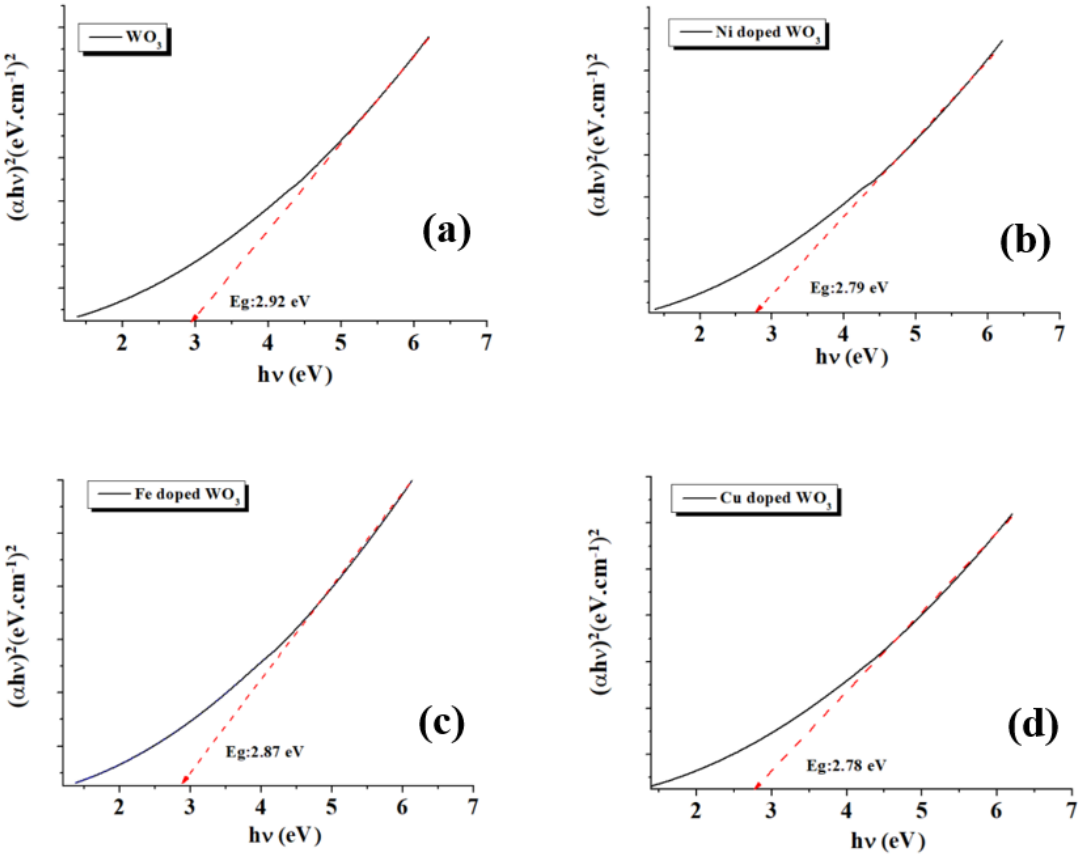

Figure 5. The optical band gap of WO_3 (a), Ni:WO_3 (b), Fe:WO_3 (c) and Cu:WO_3(d)

Other optical parameters are extinction coefficient and refractive index of WO_3, Ni:WO_3, Fe:WO_3 and Cu:WO_3 were exhibited in Figure 6 and 7, respectively. The extinction coefficient (k) is calculated as the below equation [39, 40]:

$$k = \frac{\alpha}{4\pi} \tag{3.3}$$

where α is the absorption coefficient. Figure 6 gives the k values of samples. The refractive index of the films were calculated as in the below equation [41, 42]:

$$n = \left(\frac{1+R}{1-R}\right) + \sqrt{\left(\frac{4R}{(1-R)^2} - k^2\right)} \tag{3.4}$$

where R is reflectance, and k is the extinction coefficient. These graphs exhibited that suggests a decrease in optical density with metal addition in WO_3 [43].

The dielectric constant was estimated by the below equations [42]:

$$\varepsilon = \varepsilon_r - i\varepsilon_i \tag{3.5}$$

$$\varepsilon_r = n^2 - k^2 \tag{3.6}$$

$$\varepsilon_i = 2nk \tag{3.7}$$

$$\tan\delta = \frac{\varepsilon_i}{\varepsilon_r} \tag{3.8}$$

where n is refractive index, and k is the extinction coefficient.

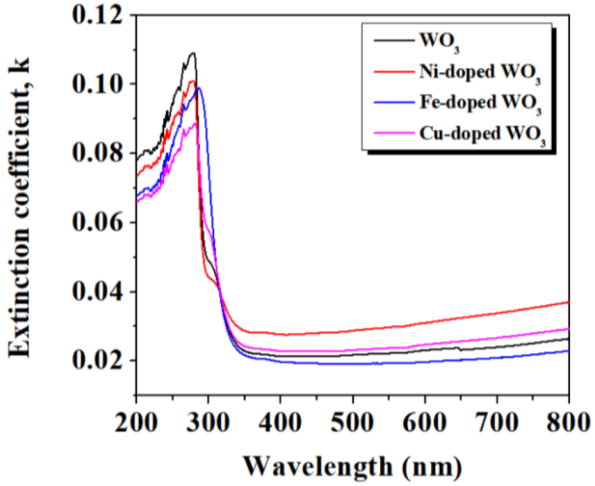

Figure 6. The extinction coefficient of pure WO_3 and M:WO_3 films

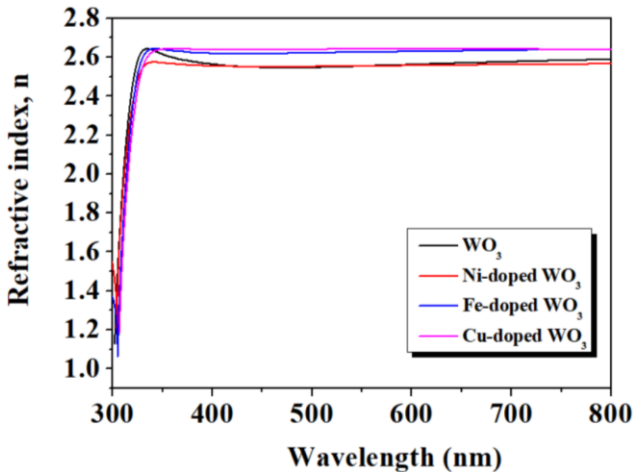

Figure 7. The refractive index of pure WO_3 and M:WO_3 films

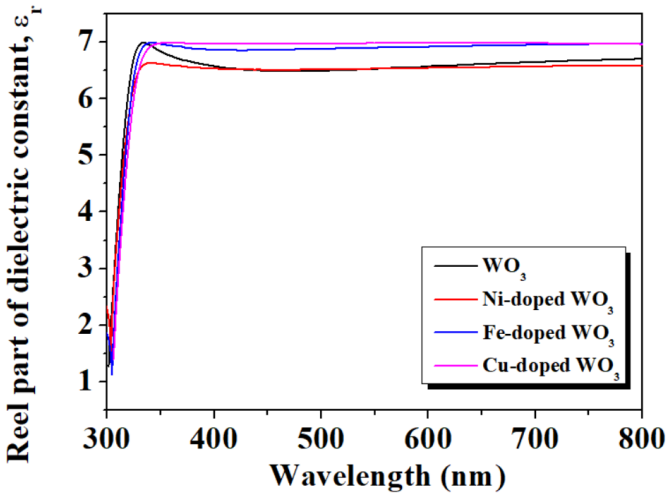

Figure 8. The reel part of dielectric constant of pure WO_3 and M:WO_3 films

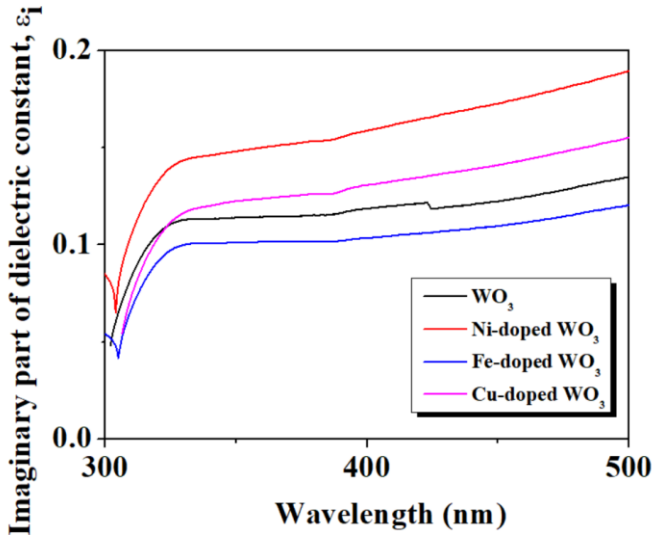

Figure 9. The imaginary part of dielectric constant of pure WO_3 and M:WO_3 films

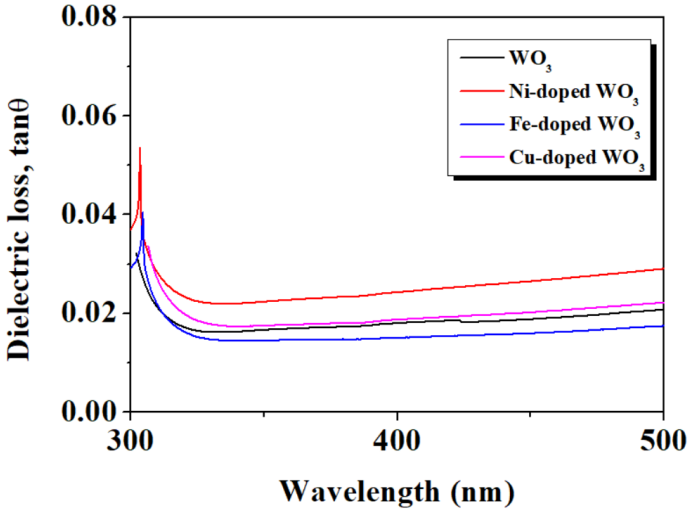

Figure 10. Dielectric loss of pure WO_3 and M:WO_3 films

The optical dielectric constant values were calculated as 6.49 , 6.51, 6.88 and 6.97 for WO_3, Ni:WO_3,Fe:WO_3 and Cu:WO_3 at the wavelength of 500 nm, respectively. From these results, the real and imaginary parts of the dielectric constant follow different patterns and the values of ε_1 are higher than those of ε_2 parts [44]. The least loss was calculated for the Fe:WO_3 sample. The dielectric constant change with hv indicates that there are complex chemical interactions dependent on the solution solubility in the investigated samples.

The current-voltage (I-V) characteristics of pure WO_3 and M:WO_3 films shown at room temperature in Figure 11. The direct current (DC) electrical characterization of each prepared pure WO_3 and M:WO_3 films was realized by measuring current-voltage (I-V) values between 0 and +2 V range. I–V curves of all samples are linear, as shown in Fig. 11 which indicates the formation of ohmic contacts between the coated films and Ag electrodes although low adhesion between ITO/coated M:WO_3. Some metal atoms are incorporated into the WO_3 films during the doping process and might form small metal clusters in the WO_3 lattice, as shown in AFM images. The conductivity of a transition metal oxide can be changed through the dopant impurity levels of electrons [23]. The resistance of samples were given in Figure 12 and calculated as 221 kΩ, 91.9 kΩ, 130 kΩ and 170 kΩ for WO_3, Ni:WO_3, Fe:WO_3 and Cu:WO_3, respectively. This slightly decrease (except for Ni:WO_3 samples) of resistance was observed by metal substitution due to the stoichiometry variation and crystal quality [45]. Since the thickness of the films is more than 100 nm, the electrical properties are independent of the film thickness, and other transmission mechanisms need to be taken into account to account for the current results [46].

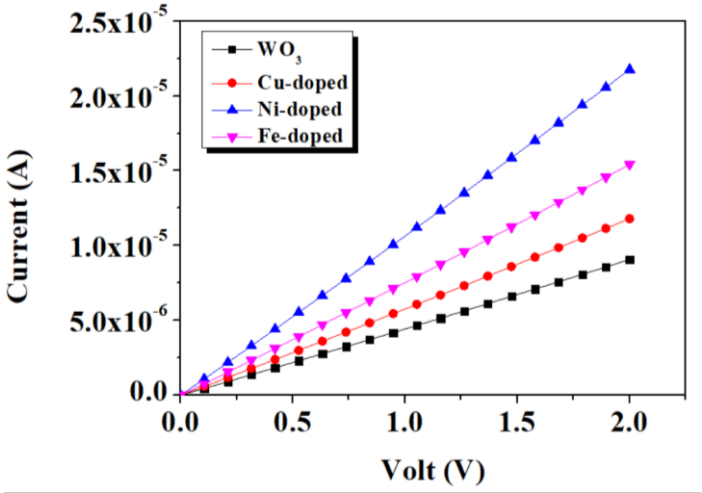

Figure 11. The current-voltage characteristics of pure WO_3 and M:WO_3 films

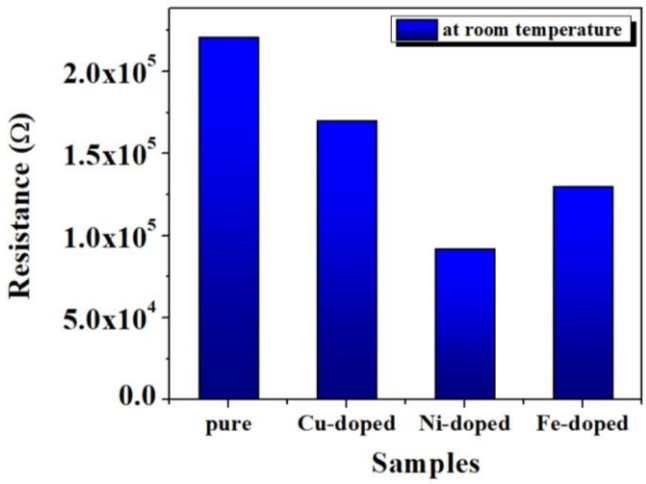

Figure 12. The resistance values of pure WO_3 and M:WO_3 films

4. Conclusion

In this study, we investigated the pure and M:WO_3 (M:Cu, Fe,Ni) films with using facile chemical bath deposition in (pH=2) acidic medium. Effect of the metal substitution on the structural, optical and electrical properties of the produced WO_3 films is studied. Structural analysis results show that all films have typical monoclinic WO_3 phase however crystal quality is low in harsh acidic medium. Optical parameters (optical absorption, emission peaks, optical band gap, optical dielectric constant) shown that the band–band transition and localized states which were produced by defects and the oxygen vacancies in metal substituted tungsten films. I-V character was linear and decrease of electrical resistance was recorded in M:WO_3 films. Each metal doping has had a different effect on both optical and electrical properties, which is due to different surface defects and lattice placement. These results shown that M:WO_3 films are proper for opto-electronic device applications.

Author Contributions

The first and third authors made experimental part. The first author designed the characterization. The second author collected data, performed the analysis, and wrote the paper with support from the third author. They all read and approved the final version of the paper.

Conflicts of Interest

All the authors declare no conflict of interest.

References

[1] N. Goel, K. Kunal, A. Kushwaha, M. Kumar, *Metal oxide semiconductors for gas sensing*, Engineering Reports 5 (6) (2023) e12604.

[2] S. A. Beknalkar, A. M. Teli, J. C. Shin, *Current innovations and future prospects of metal oxide elecrospun materials for supercapacitor technology: A review*, Journal of Materials Science & Technology 166 (2023) 208–233.

[3] K. Valadi, S. Gharibi, R. Taheri-Ledari, *Metal oxide electron transport materials for perovskite solar cells: A review*, *Environmental Chemistry Letters* 19 (2021) 2185–2207.

[4] M. Zhou, S. Wang, M. Qiu, B. Hu, G. Wang, Y. Lu, *Recent advances in the removal of U(VI) by magnetic metal oxides*, Journal of Molecular Liquids 385 (2023) 122295.

[5] S. Masroor, *Chapter 4 - Basics of metal oxides: properties and applications*, Inorganic Anticorrosive Materials (2022) 85-94.

[6] M. Tang, J. Shanga, Y. Zhang, *Oxygen vacancy and doping atom effect on electronic structure and optical properties of Cd_2SnO_4*, RSC Advances 8 (2) (2018) 640–646.

[7] F. Özütok, E. Yakar, *Optical and electrochemical properties of PB-ZnO and PB-ZnO/MWCNT nanocomposite films deposited by chemical bath*, Journal of New Materials for Electrochemical Systems 21 (2) (2018) 119–126.

[8] B. Zhang, Z. An, M. Li, L.-H. Guo, *Synthesis, functionalization and photoelectrochemical immunosensing application of WO_3-based semiconductor materials*, TrAC Trends in Analytical Chemistry 165 (2023) 117149.

[9] M. Razzaq, M. J. Khan, Z. Imran, M. Ahmad, S. Rasool, M. Rehan, S. Iqbal, M. A. R. Anjum, S.

Mehboob, M. Saifullah, *Enhanced electrochemical performance of WO3 thin films prepared from polyvinyl alcohol-modified nanoparticle ink*, Solid State Communications 397 (2023) 116246.

[10] M. Ikram, S. Rasheed, A. M. Afzal, N. A. Shad, Y. Javed, A. Mohyuddin, T. Alomayri, M. M. Sajid, A. Almahri, D. Hussain, *Ultrasensitive V doped WO_3 1D nanorods heterojunction photodetector with pronounced photosensing activities*, Journal of Alloys and Compounds 909 (2022) 164753.

[11] K. Sutanto, N. R. Al Amin, C.-H. Chen, D. Luo, C. Chen, S. Biring, C. Lee, S. Liu, *Vacuum deposited WO_3/Al/Al:Ag anode for efficient red organic light-emitting diodes*, Organic Electronics 103 (2022) 106454.

[12] J. Y. Zheng, Q. Sun, J. Cui, X. Yu, S. Li, L. Zhang, S. Jiang, W. Ma, R. Ma, *Review on recent progress in WO3-based electrochromic films: preparation methods and performance enhancement strategies*, Nanoscale 15 (1) (2023) 63–79.

[13] Z. Xin-Ping, L. Gao, H. Zhang, Y. Peng, X. Zhang, Q. Wang, H. Zhang, *Defect Engineering of Ultrathin WO3 Nanosheets: Implications for Nonlinear Optoelectronic Devices*, ACS Applied Nano Materials 5 (1) (2022) 1169–1177.

[14] R. A. Phokojoe, S. V. Motloung, T. E. Motaung, M. A. Kebede, H. C. Swart, L. F. Koao, *Effect of annealing time on copper selenide thin films prepared by chemical bath deposition*, Physica B: Condensed Matter 666 (2023) 415112.

[15] Z. Yao, P. Li, X. Liu, *Growth regulation of WO_3 film by H2C2O4 during chemical bath deposition*, Journal of Crystal Growth 601 (2023) 126947.

[16] F. Sarf, I. Karaduman, A. Ajjaq, E. Yakar, A. O. Çağırtekin, S. Acar, *Varying electrical and dielectric properties of Ni:SnO2 films by MWCNTs and GNPs coating*, Physica Scripta 97 (2) (2022) 25805-25815.

[17] Ü. Ö. A. Arıer, *Effects of doping ratios on the electrochromic features of WO3-VO2 nano-composite films*, Optik 262 (2022) 169195.

[18] X. Dong, Y. Wei, J. Gao, X. Liu, L. Zhang, Y. Tong, Y. Lu, *Efficient charge transfer over Cu-doped hexagonal WO_3 nanocomposites for rapid photochromic response*, Journal of Photochemistry and Photobiology A: Chemistry 425 (2022) 113716.

[19] H. Liu, J. Zhou, L. Yu, Q. Wang, B. Liu, P. Li, Y. Zhang, *High-sensitivity SO_2 Gas Sensor based on noble metal doped WO_3*, nanomaterials, International Journal of Electrochemical Science 16 (12) (2021) 211240.

[20] Z. Chen, J. Li, S. Wang, J. Zhao, J. Liu, J. Shen, C. Qi, P. Yang, *Structure-property-performance relationship of transition metal doped WO3 mixed oxides for catalytic degradation of organic pollutants*, Chemosphere 316 (2023) 137797.

[21] O. E. Gülen, E. Yakar, F. Sarf, *Investigation of microstructural and intrinsic defect states of facile synthesized WO3 film*, Bilge International Journal of Science and Technology Research 6 (1) (2022) 16–19.

[22] J. Velevska, N. Stojanov, M. Pecovska-Gjorgjevich, M. Najdoski, *Electrochromism in tungsten oxide thin films prepared by chemical bath deposition*, Journal of Electrochemical Science and Engineering 7 (1) (2017) 27–37.

[23] I. Karaduman Er, S. Uysal, A. Ateş, S. Acar, *Some sol–gel processing parameters effect on the properties of dip coated TiO_2 thin films*, *J Mater Sci: Mater Electron* 34 (2023) Article Number 1512 19 pages.

[24] H. Lincy P. C. J. Prabakar, S. J. Gnanamuthu, I. J. D. Ebenezar, *Ammonia sensing performance of Ni doped-WO3 nano particles prepared by simple hydrothermal method at room temperature*, Materials Today: Proceedings 80 (2) (2023) 958-964.

[25] C. Lu, M. H. Hon, C. Kuan, I. Leu, *Preparation of WO3 nanorods by a hydrothermal method for electrochromic device*, Japanese Journal of Applied Physics 53 (2014) 06JG08 1–5.

[26] R. Solarska, A. Królikowska, J. Augustyński, Silver nanoparticle induced photocurrent enhancement at WO3 photoanodes. Angewandte Chemie International Edition 49 (43) (2010) 7980-3.

[27] V. S. Kavitha, V. Biju, K. G. Gopchandran, R. Praveena, C. K. Jayasankar, W. Mekprasart, K. Boonyarattanakalin, W. Pecharapa, V. P. M. Pillai, *Tailoring the emission behavior of WO_3 thin films by Eu^{3+} Ions for light-emitting applications*, Nanomaterials 13 (1) (2023) 7.

[28] M. F. Al-Kuhaili, Q. A. Drmosh, *Investigating the structural and optoelectronic properties of co-sputtered Fe-doped WO_3 thin films and their suitability for photocatalytic applications*, Materials Chemistry and Physics 281 (2022) 125897.

[29] H. Liyanaarachchi, C. Thambiliyagodage, C. Liyanaarachchi, U. Samarakoon, *Efficient photocatalysis of Cu doped TiO_2/g-C_3N_4 for the photodegradation of methylene blue*, Arabian Journal of Chemistry 16 (6) (2023) 104749.

[30] A. Lushchik, M. Kirm, Ch. Lushchik, I. Martinson, H. Zimmerer, *Luminescence of free and self-trapped excitons in wide-gap oxides*, Journal of Luminescence 87 (2000) 232–234.

[31] P. Kumar, M. Singh, G. B. Reddy, *Core–shell WO_3–WS_2 nanostructured thin films via plasma assisted sublimation and sulfurization*, ACS Applied Nano Materials 2 (3) (2019) 1691–1703.

[32] T. Kuechle, S. Klimmer, M. Lapteva, T. Hamzayev, A. George, A. Turchanin, T. Fritz, C. Ronning, M. Gruenewald, G. Soavi, *Tuning exciton recombination rates in doped transition metal dichalcogenides*, Optical Materials: X 12 (2021) 100097.

[33] Y. S. Zou, Y. C. Zhang, D. Lou, H. P. Wang, L. Gu, Y. H. Dong, K. Dou, X. F. Song, H. B. Zeng, *Structural and optical properties of WO_3 films deposited by pulsed laser deposition*, Journal of Alloys and Compounds 583 (2014) 465–470.

[34] K. M. Reddy, S. V. Manorama, A. R. Reddy, *Bandgap studies on anatase titanium dioxide nanoparticles*, Materials Chemistry and Physics 78 (1) (2003) 239–245.

[35] M. Devi, M. R. Panigrahi, *Synthesis and characterization of Mg doped TiO_2 thin film for solar cell application,* International Journal of Engineering & Applied Sciences 7 (2015) 1–7.

[36] I. Karaduman Er, F. Sarf, E. Yakar, *Investigation of H_2S gas sensing performance of Ni:WO_3 films at room temperature: nickel precursor effect*, *Journal of Materials Science: Materials in Electronics* 33 (2022) 3397–3410.

[37] Deepika, D. Gupta, V. Chauhan, S. K. Sharma, S. Kumar, R. Kumar, *Effect of gamma irradiation induced modifications in tungsten oxide thin films and their potential applications,* Indian Journal of Engineering and Materials Sciences 30 (3) (2023) 409–415.

[38] D. Gupta, V. Chauhan, A. Mahajan, R. Gupta, S. A. Ali, R. Kumar, *Influence of gamma radiation on optical, structural and surface morphological properties of WO_3 thin films grown by RF sputtering*, Radiation Physics and Chemistry 2022 (2022) 110554.

[39] R. Suresh, V. Ponnuswamy, R. Mariappan, *Influence of mole concentration on the optical properties of nebulized spray coated CeO_2 thin films*, Journal Optics 44 (2015) 203–209.

[40] M. N. Solovan, P. D. Maryanchuk, V. V. Brus, O. A. Parfenyuk, *Electrical and Optical Properties of TiO_2 and TiO_2: Fe thin films*, Inorganic Materials 48 (10) (2012) 1026–1032.

[41] A.-S. Gadallah, M. M. El-Nahass, *Structural, Optical Constants and Photoluminescence of ZnO Thin Films Grown by Sol-Gel Spin Coating*, Advances in Condensed Matter Physics 2013 (2013) Article ID 234546 11 pages.

[42] S. Tekin, I. Karaduman Er, *The structural, morphological, optical and gas-sensing properties of Mn_3O_4 thin films grown by successive ionic layer adsorption and reaction technique*, Journal of Materials Science: Materials in Electronics 33 (2022) 14519–14534.

[43] A. Rydosz, K. Dyndał, K. Kollbek, W. Andrysiewicz, M. Sitarz, K. Marszałek, *Structure and optical properties of the WO_3 thin films deposited by the GLAD magnetron sputtering technique*, Vacuum 177 (2020) 109378.

[44] E. M. Ngigi, P. S. Nomngongo, J. C. Ngila, *Synthesis and application of Fe-doped WO_3 nanoparticles for photocatalytic degradation of methylparaben using visible–light radiation and H_2O_2,* Catalysis Letters 149 (2019) 49–60.

[45] V. V. Ganbavle, G. L. Agawane, A. V. Moholkar, J. H. Kim, K. Y. Rajpure, *Structural, Optical, Electrical, and Dielectric Properties of the Spray-Deposited WO_3 Thin Films*, Journal of Materials Engineering and Performance 23 (2014) 1204–1213.

[46] M. Regragui, V. Jousseaume, M. Addou, A. Outzourhit, J. C. Bernéde, B. El Idrissi, *Electrical and optical properties of WO_3 thin films*, Thin Solid Films, 397 (1–2) (2001) 238-243.